ELSEVIER

Journal of Power Sources 68 (1997) 91–98

JOURNAL OF POWER SOURCES

Recent studies on the correlation between surface chemistry, morphology, three-dimensional structures and performance of Li and Li–C intercalation anodes in several important electrolyte systems

D. Aurbach *, A. Zaban, Y. Ein-Eli, I. Weissman, O. Chusid, B. Markovsky, M. Levi, E. Levi, A. Schechter, E. Granot

Department of Chemistry, Bar-Ilan University, Ramat Gan, 52900 Israel

Accepted 21 December 1996

Abstract

This paper reviews some advances in the comparative study of lithium and graphite electrodes in a large matrix of solvents, salts and additives. The major purpose of this work was to support R&D of lithium metal and Li-ion batteries by understanding the correlation between the anode's performance, its morphology and three-dimensional structure upon cycling, interfacial electronic properties and the surface chemistry. The emphasis was on the use of the most sophisticated novel spectroscopic tools in conjunction with standard electrochemical techniques. These included in situ and ex situ Fourier-transform infrared spectroscopy (FT-IR) and X-ray difraction (XRD), impedance spectroscopy and atomic force microscopies (EIS and AFM, respectively), X-ray photospectroscopy (XPS), energy dispersive analysis of X-rays (EDAX) and electrochemical quartz crystal microbalance (EQCM). Major achievements included: (i) analysis of the surface reactions which are taking place on both the lithium and the carbon electrodes which form surface films that control the electrochemical behaviour in many electrolyte systems of interest; (ii) successful and useful application of AFM and EQCM in order to study the surface film formation and Li-deposition processes; (iii) understanding the correlation between the reversibility and stability of graphite electrodes in Li-intercalation processes and their surface chemistry, and (iv) finding an interesting correlation between the three-dimensional structure of graphite electrodes, the diffusion coefficient of Li^+ and their voltammetric behaviour in Li-intercalation processes. © 1997 Elsevier Science S.A.

Keywords: Lithium; Intercalation; Surface chemistry; Analytical techniques; Cyclic voltammetry

1. Introduction

It is generally accepted that the performance of all lithium batteries including lithium metal–liquid electrolyte, lithium metal–polymer electrolyte and all types of Li-ion battery systems depends on the surface chemistry developed on the anode/electrolyte interface system. This surface chemistry is inevitable due to the fact that lithium or carbon intercalated with lithium is reactive with all polar aprotic solvents, salt anions and many of the commonly used conducting polymers. The reaction between the anode material and the various components of the surface films usually produces ionic compounds which are lithium salts. These may include lithium halides, oxides, hydroxide, nitride, carbonates (both organic and inorganic), alkoxides, arsenides, phosphides, etc. These lithium salts precipitate as surface films on the anodes, passivate them and usually behave as a solid electrolyte (Li-ion conducting, electronic insulating) interphase. The composition and three-dimensional (3D) structure of this interphase formed in the various electrolyte systems on the lithium anodes (Li metal, Li–C, Li alloys, etc.) determine their passivation, the uniformity of lithium dissolution/deposition and the chance for detrimental interactions between carbon materials and components of the electrolyte solutions during lithium intercalation.

As already reported in Refs. [1–5], the same surface chemistry is developed on lithium metal, carbon intercalated with lithium and noble metal polarized to low potentials in many lithium battery electrolyte solutions. In view of this, a comparative study of these three types of electrodes may be very helpful in the understanding of the connection between elec-

* Corresponding author. Fax: 972 3 5351250.

PII S0378-7753(97)02575-5

trolyte solution compositions and the performance of lithium or Li–C anodes in the battery systems.

In this paper we report briefly on our recent studies of lithium, Li–C and noble metal electrodes in several important relevant liquid electrolyte solutions. The emphasis was on the use of the most advanced spectroscopic techniques in conjunction with high level electrochemical tools. For the study of lithium electrodes in solutions, ex situ and in situ Fourier-transform infrared (FT-IR), X-ray photospectroscopy (XPS) impedance spectroscopies, energy dispersive analysis of X-rays (EDAX), scanning electron microscopy (SEM) and atomic force microscopy (AFM) have been used in conjunction with standard electrochemical techniques for a rigorous study of the correlation between the surface chemistry, morphology, electronic properties and lithium-cycling efficiency. For the study of Li–C electrodes, FT-IR, EDAX, XPS and in situ XRD have been used in conjunction with impedance spectroscopy, slow scan cyclic voltammetry (μV/s) and potentiostatic intermittent titration (PITT). A most important channel of information was obtained by the study of non-active metal electrodes (Pt, Au, Ni, Cu) polarized to low potentials in the electrolyte solutions. These electrodes develop, at low potentials in all the lithium battery electrolyte solutions, surface films which are very similar to those developed on both Li and Li–C electrodes [6]. The study of these films on the noble metals provides useful information on their structure and stability and enables a comparison amongst the various electrolyte solutions, in terms of passivating properties of the surface films formed and the correlation between the solution composition (solvent, salt additives, contaminants) and the properties of the surface films. In situ FT-IR, EQCM, impedance spectroscopies and AFM were applied in conjunction with cyclic voltammetry and chronoamperometry for the study of noble metal electrodes in solutions. A large matrix of solvents, salts and additives was studied including alkyl carbonates (propylene carbonate (PC), ethylene carbonate (EC), dimethyl carbonate (DMC), diethyl carbonate (DEC)), ethers (2-methyltetrahydrofuran (2Me-THF), tetrahydrofuran (THF), glymes, 1,3-dioxane and 1,4-dioxane, 1,3–dioxolane) and esters (methyl formate, γ-butyrolactone), and lithium salts such as $LiClO_4$, $LiAsF_6$, $LiN(SO_2CF_3)_2$, $LiC(SO_2CF_3)_2$, $LiSO_3CF_3$, LiBr, LiI and $LiBF_4$ and $LiPF_6$ from several suppliers.

2. Experimental

Application of FT-IR, in situ XRD, impedance spectroscopy, SEM, EDAX and EQCM for the study of the above systems has already been described in Refs. [1–10]. The application of AFM to these systems is described in Ref. [11]. Special attention has been paid to contamination problems in the solutions during the spectroscopic measurements. Transfer systems were built for ex situ techniques and special cells were constructed for the in situ techniques. The solvents were obtained from Tomiyama, Burdick and Jackson Grant Chemicals and Aldrich as already reported [1–10]. The above-mentioned ethers, methyl formate, DMC and DEC were further distilled under high purity argon prior to use. EC and PC could be used as received from Tomiyama. $LiAsF_6$ (Lithco), $LiPF_6$ (Tomiyama, Hashimoto), $LiBF_4$ (Tomiyama), $LiClO_4$ (Tomiyama) and $LiC(SO_2CF_3)_3$ (Covalent) could be used as received. $LiN(SO_2CF_3)_3$ (3 M) had to be dried before use (vacuum oven, 10^{-2} torr, 90 °C, 48 h).

3. Results and discussion

3.1. Lithium–metal electrodes

Ethers are the most promising solvents for rechargeable lithium battery systems with lithium metal anodes. There are several combinations such as 2-Me-THF/THF/methyl furan and $LiAsF_6$ in which the Li–TiS_2 systems provide prolonged cycle life, and indeed lithium morphology is very smooth during charge/discharge cycling in these solutions. The spectroscopic studies revealed that the ether linkage is attacked and cleaved on the lithium surface to form lithium alkoxide

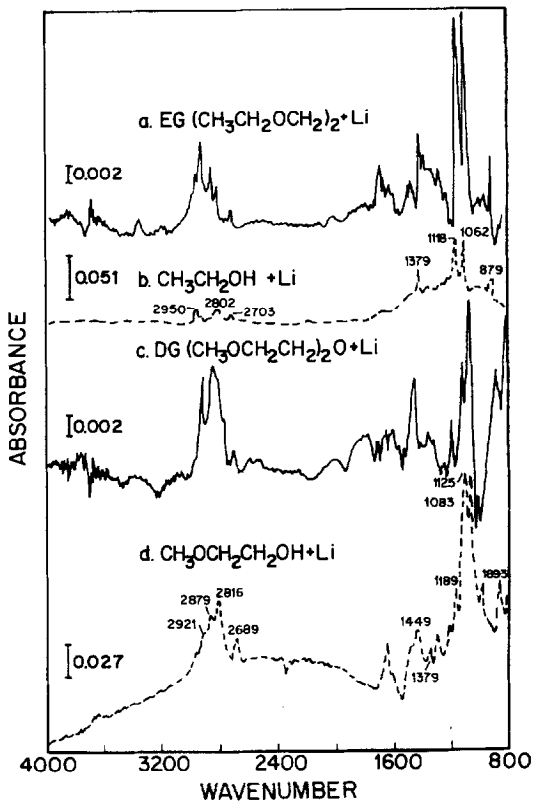

Fig. 1. FT-IR spectra of the lithium electrode prepared and stored for several weeks in diethylglyme (CH_3CH_2–OCH_2CH_2–O–CH_2CH_3) and diglyme ($CH_3OCH_2CH_2)_2O$. Spectra of CH_3CH_2OLi and $CH_3OCH_2CH_2OLi$ (as thin films on Li) are also shown for comparison.

films. A typical spectral analysis which leads to this conclusion (including comparison with reference spectra of the lithium alkoxides on lithium) is shown in Fig. 1. This figure shows FT-IR spectra measured (ex situ, external reflectance mode) from lithium surfaces prepared fresh and stored for a few weeks in two linear ethers: ethyl glyme $(CH_3CH_2OCH_2)_2$ (EG) and diglyme $(CH_3OCH_2CH_2)_2O$ (DG). Special care has been taken in these experiments to avoid any possible secondary reactions between the lithium surfaces or the surface species formed on it with atmospheric components (such as H_2O and CO_2 to which lithium and lithium surface species are sensitive at the ppm level [7]). Spectra of the alkoxides CH_3CH_2OLi and $CH_3OCH_2CH_2$–OLi prepared as thin films on lithium (by reacting lithium with the parent alcohols) are also presented for a comparison. This comparison is straightforward and proves that EG reacts with lithium to form surface lithium ethoxide, and that DG reacts on the active metal surface to form Li/2-methoxy-ethoxide. These results are the clearest that we have ever obtained after obvious identification of specific alkoxides formed by reduction of ether solvents on lithium. When the salt used is $LiAsF_6$, the surface films also comprise LiF and Li_xAsF_y species (EDAX, XPS, in situ FT-IR). We therefore conclude that when the lithium surfaces are protected by a combination of LiF and lithium alkoxide films and the lithium is doped by arsenic (As°) and arsenic compounds (possible Li_3As, Li_2AsF and $LiAsF_2$), it induces uniform and smooth lithium deposition (which leads to the high lithium cycling efficiency measured). A comparative study of ethereal solutions of all the other salts from the above list shows that $LiBF_4$ and $LiPF_6$ are too acidic to form stable solutions, and that $LiClO_4$, $LiSO_3CF_3$, $LiN(SO_2CF_3)_2$ and $LiC(SO_2CF_3)_3$ are too reactive with lithium. The variety of the salt anion reduction products which precipitate on the lithium surfaces in these cases form heterogeneous surface films which induce a non-uniform and highly dendritic lithium deposition. The study of lithium anodes in alkyl carbonates is very important for the understanding of the more complicated Li–C systems where these solvents are highly important (due to their apparent stability and relatively wide electrochemical window which is good for the 4 V cathodes). Especially interesting is the comparison between DMC–EC and DEC–EC solutions and between $LiAsF_6$ and $LiClO_4$, $LiN(SO_2CF_3)_2$ and the acidic salts $LiBF_4$ and $LiPF_6$. The lithium surface chemistry in the above systems was analysed by FT-IR, EDAX and XPS. EC is reduced to $ROCO_2Li$, probably $(CH_2OCO_2Li)_2$ [12] and DMC and DEC are reduced to both ROLi and $ROCO_2Li$ (R = CH_3 - or CH_3CH_2 - for DMC or DEC, respectively). Fig. 2 compares several FT-IR spectra measured (ex situ, external reflectance mode) from lithium electrodes prepared fresh and stored for a few days in various EC–DMC solutions, and in fact clearly reflects the surface chemistry of lithium electrodes in these solutions, as summarized above.

Fig. 2(a) and (b) relates to 1 M $LiAsF_6$ solutions of two solvent ratios (EC–DMC, in 2:1 and 1:3 ratios, respectively). Both spectra are typical of a combination of surface $(CH_2OCO_2Li)_2$ [12], Li_2CO_3 [12] residual EC and Li_xAsF_y compounds as indicated by the peak assignments appearing in the figure. A comparison of these two spectra with an FT-IR spectrum of a combination of CH_3OCO_2Li and CH_3OLi

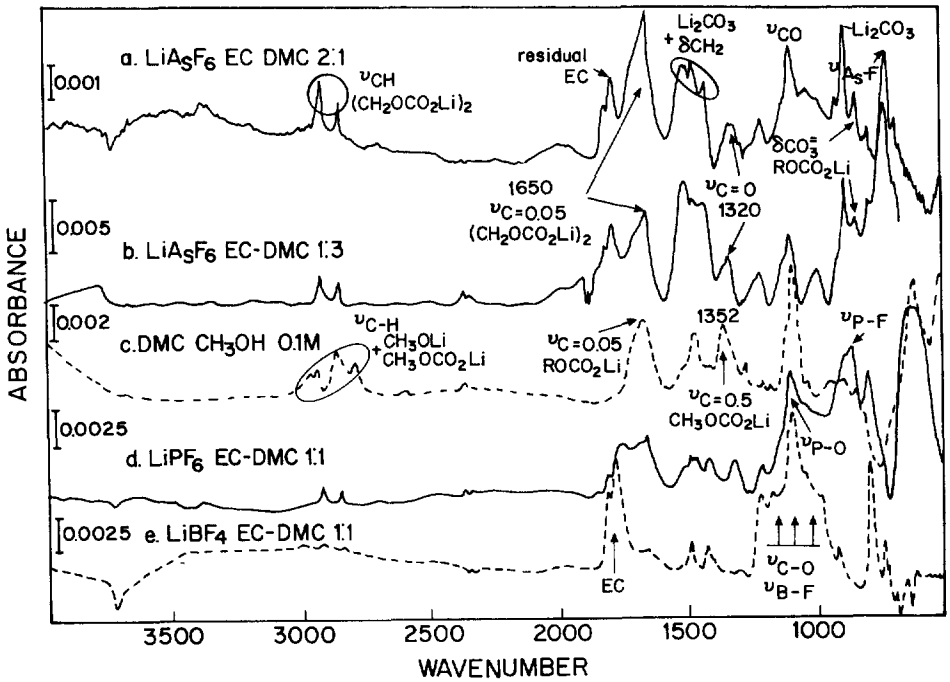

Fig. 2. FT-IR spectra of lithium electrodes prepared and stored for three days in EC–DMC solutions of 1 M $LiAsF_6$ and 1 M $LiPF_6$ and $LiBF_4$ as indicated. A spectrum of lithium electrode prepared and stored in DMC containing 0.1 M CH_3OH is also presented for a comparison.

(deposited as a thin film on a reflective lithium surface by reacting lithium with DMC containing CH_3OH contamination) reveals that none of these species are major constituents in the surface films formed on lithium in EC–DMC mixtures (compare the υ_{C-H} region around 3000–2700 cm^{-1} and the $\upsilon_{C=O,S}$ bands of the $ROCO_2Li$ appearing in the 1360–1300 range), Fig. 2(c).

Fig. 2(d) and (e) relates to $LiPF_6$ and $LiBF_4$ solutions, respectively, and are quite different from those of Fig. 2(a) and (b). Fig. 2(c) has P–O and P–F absorption bands (1080–1020, 850 cm^{-1}, respectively), as the dominant features (in addition to relatively small $ROCO_2Li$ peaks as indicated), and Fig. 2(e) lacks carbonate peaks and has its strongest absorption bands in the 1200–950 range (in addition to peaks of residual EC as indicated). It should be stressed that FT-IR spectra measured from similar lithium electrodes after being stored for a short period of time revealed that the initial surface species formed are indeed the $ROCO_2Li$ compounds.

These spectral results demonstrate the ageing processes taking place in $LiPF_6$ and $LiBF_4$ solutions which solubilize the carbonates initially formed and replace them with salt reduction products. Especially intriguing is the surface chemistry developed in $LiBF_4$ solutions during storage. However, a detailed discussion on this is beyond the scope of this paper. The DEC reduction products are soluble in the mother solvent while DMC reduction products are not. In mixtures of EC–DMC or EC–DEC the lithium surface chemistry is dominated by EC reduction. However, in the former mixture CH_3OLi and CH_3OCO_2Li may also be present on lithium in the surface films as minor constituents, while in EC–DEC only the EC reduction product is stable as a surface compound. The above solvent reactions indeed determine the lithium surface chemistry in $LiAsF_6$ or $LiClO_4$ solutions. $LiPF_6$ or $LiBF_4$ solutions contain HF contamination which solubilizes the carbonates and replaces them with LiF. This ageing process increases considerably the interfacial resistance of lithium electrodes in these solutions because the LiF surface films are more resistant to lithium migration than the carbonate films. The higher stability of lithium in EC–DMC compared with EC–DEC mixture is reflected by impedance measurements' electron microscopy and lithium cycling efficiency studies. Lithium interfacial resistance is much lower and stable upon storage in EC–DMC. Upon charge/discharge cycling, lithium morphology is much smoother and lithium cycling efficiency is higher in EC–DMC compared with EC–DEC solutions. The XPS studies further prove that in addition to the ($-OCO_2Li$) functional group, the surface films also contain Li–C bonds. (Hence, it is possible that when DMC is reduced to CH_3OCO_2Li on lithium the co-product $-CH_3$ is further reduced to CH_3Li). These studies of lithium electrodes and their resultant conclusions obviously reflect on the choice of electrolyte solutions for Li-ion batteries. Based on the above studies, Scheme 1 summarizes major surface reactions of solvent and salts with lithium and Li–C, which form surface films.

1. Possible Reduction Patterns of Alkyl Carbonates on Li and carbon

a) $PC + 2e^- + 2Li \rightarrow Li_2CO_3\downarrow + CH_3CH=CH_2\uparrow$

$2PC \xrightarrow{Li^+,e^-} CH_3\dot{C}HCH_2OCO_2^-Li^+ \; (PC^{\bullet -}Li^+)$

b) $CH_3\dot{C}HCH_2OCO_2Li + H^\bullet \rightarrow CH_3CH_2CH_2OCO_2Li$

c) $2CH_3\dot{C}HCH_2OCO_2Li \xrightarrow{?} CH_3-\underset{\displaystyle CH_3-CH-CH_2OCO_2Li}{\overset{|}{CH}}-CH_2OCO_2Li$

d) $\longrightarrow CH_3CH(OCO_2Li)CH_2OCO_2Li\downarrow + CH_3CH=CH_2\uparrow$

e) $2EC \xrightarrow{2e^-,2Li^+} (CH_2OCO_2Li)_2\downarrow + CH_2=CH_2\uparrow$

f) $2EC \xrightarrow{2e^-,2Li^+} LiOCO_2(CH_2)_4OCO_2Li$?

g) $Li_2O + EC \longrightarrow LiOCH_2CH_2OCO_2Li$?

h) $(DMC)\,CH_3OCOCH_3 + e^- + Li^+ \longrightarrow CH_3OCO_2Li\downarrow + CH_3^\bullet$ or $CH_3OLi\downarrow + CH_3OCO^\bullet$

i) $2ROCO_2Li + H_2O \longrightarrow Li_2CO_3 + 2ROH + CO_2$

j) $R^\bullet + Li^\circ \longrightarrow R-Li$

2. Possible ether reduction patterns on Li and carbon

a) $R\text{-}O\text{-}R` + e^- + Li^+ \rightarrow R`OR^{\bullet -}Li^+$

b) $R`OR^{\bullet -}Li^+ \rightarrow ROLi + R`^\bullet$ or $R`OLi + R^\bullet$

c) $R^\bullet \xrightarrow{H^\bullet} RH$ or $2R^\bullet \rightarrow R_2$ or $R^\bullet \xrightarrow{Li^\circ} RLi$

d) (EG) $CH_3CH_2OCH_2CH_2OCH_2CH_3 + Li^+ + e^- \rightarrow$

$CH_3CH_2OLi\downarrow + {}^\bullet CH_2CH_2\text{-}OCH_2CH_3$ or

$CH_3CH_2{}^\bullet + CH_3CH_2OCH_2CH_2OLi\downarrow$

e) $1-3Dioxolane + e^- + Li^+ \longrightarrow \dot{C}H_2CH_2OCH_2OLi$ (major)

or $\dot{C}H_2OCH_2CH_2OLi$

f) $^\bullet CH_2CH_2OCH_2OLi \xrightarrow{H^\bullet} CH_3CH_2OCH_2OLi\downarrow$

or $CH_3CH_3\uparrow + HCO_2Li\downarrow$

g) $^\bullet CH_2CH_2OCH_2OLi \xrightarrow{Li^\circ} LiCH_2CH_2OCH_2OLi$

h) $ROLi + nDN \xrightarrow{\text{polymerization}} R-(OCH_2CH_2-OCH_2)_n OLi\downarrow$

3. Possible $LiBF_4$, $LiPF_6$ and $LiAsF_6$ Reduction Patterns (Li, carbon)

a) $LiAsF_6 + 2Li^+ + 2e^- \rightarrow 3LiF\downarrow + AsF_3$ (sol)

b) $AsF_3 + 2 \times Li^+ + 2 \times e^- \rightarrow Li_xAsF_{3-x}\downarrow + XLiF\downarrow$

c) $PF_6^- + 3Li^+ + 2e^- \rightarrow 3LiF\downarrow + PF_5$

d) $LiPF_6 \longrightarrow LiF + PF_5$

e) $PF_5 + H_2O \rightarrow PF_3O + 2HF$

f) $PF_5 + 2 \times Li^+ + 2 \times e^- \rightarrow Li_xPF_{5-x}\downarrow + XLiF\downarrow$

g) $PF_3O + 2X\,Li^+ + 2 \times e^- \rightarrow Li_xPF_{3-x}O\downarrow + XLiF\downarrow$

h) $BF_4^- \xrightarrow{Li^+,e^-} LiF\downarrow, Li_xBF_y\downarrow$ (in general)

i) $ROCO_2Li\downarrow, Li_2CO_3\downarrow \xrightarrow{HF_{(sol)}} LiF\downarrow + ROCO_2H_{(sol)}, H_2CO_{3(sol)}$

4. Possible $LiN(SO_2CF_3)_2$ and $LiC(SO_2CF_3)_3$ Reduction Patterns (Li, carbon)

a) $LiN(SO_2CF_3)_2 + ne^- + nLi^+ \rightarrow Li_3N + Li_2S_2O_4 + LiF + C_xF_yLi_z$

b) $LiN(SO_2CF_3)_2 + 2e^- + 2Li^+ \rightarrow Li_2NSO_2CF_3 + CF_3SO_2Li$

c) $Li_2S_2O_4 + 6e^- + 6Li^+ \rightarrow 2Li_2S + 4Li_2O$

d) $LiC(SO_2CF_3)_3 + 2e^- + 2Li^+ \rightarrow Li_2C(SO_2CF_3)_2 + LiSO_2CF_3$, etc.

e) $Li_2S_2O_4 + 4e^- + 4Li^+ \rightarrow Li_2SO_3 + Li_2S + Li_2O$

Scheme 1.

3.2. Morphology of lithium electrodes

The traditional tool for morphological studies of electrodes is SEM; with respect to lithium electrodes, this method has the following disadvantages:

1. The measurements are performed ex situ after the electrodes being washed, evacuated and transferred from the electrochemical environment (solution under highly pure argon) to the microscope (vacuum of 10^{-5}–10^{-6} torr). This procedure may lead to reactions of the sensitive lithium electrodes with reactive atmospheric components (e.g. O_2, N_2, H_2O) which change the electrodes' surface. In addition, washing the electrode prior to transfer to the microscope may change the electrode's morphology in cases where it is highly dendritic.
2. The lithium surfaces are covered with surface films which are electronic insulators. As such, they cause charging of the electrode by the electron beam and this phenomenon considerably decreases the resolution of the SEM measurements and in many cases limits it to the μm scale.

The development of scanning probe microscopies such as AFM [13] open new horizons for in situ morphological studies of electrochemical systems at very high resolutions (even at the atomic scale [13]). It was possible to distinguish between different morphologies of lithium deposition processes in different solutions. For instance, lithium deposition in $LiPF_6$/PC solutions is more uniform than in $LiClO_4$/PC solutions and correlates well with the different surface chemistry developed in these two solutions [11].

These preliminary studies encourage the systematic use of AFM for in situ morphological studies of lithium electrodes in all the electrolyte solutions of interest. The major benefit of these studies is the understanding of the correlation between the solution composition and the morphology of lithium deposition/dissolution processes. In recent publications [11,14] we reported on the in situ study of lithium deposition processes using AFM, and the cell and the methodology were described in detail [11]. In the present review we summarize a few major conclusion drawn from this study:

1. the use of AFM enables us to follow the formation of porous surface films on noble metal electrodes when polarized to low potentials in commonly used electrolyte solutions, and
2. it was possible to follow lithium deposition processes at a sub-micrometer scale with no detrimental inference by the AFM tip with the morphology of the soft lithium deposits.

3.3. Noble metal electrodes in solutions

The basic voltammetric behaviour of noble metal electrodes such as gold in ether, ester or alkyl carbonate solvents containing lithium salt from the above list (except for LiBr or LiI where salt reduction is not relevant) is similar and is described schematically in Fig. 3, together with some results

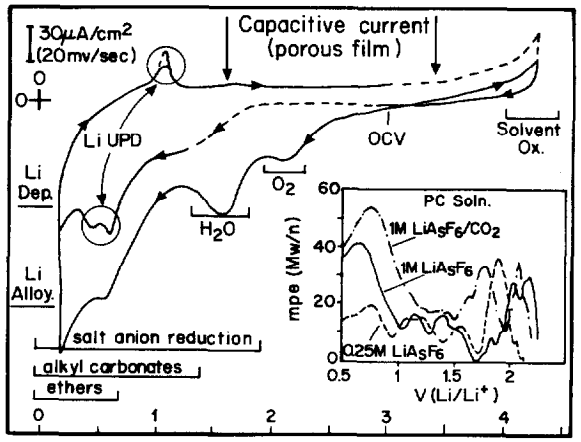

Fig. 3. A typical schematic cyclic voltammogram of ether, ester or alkyl carbonate solvent (except DEC) containing lithium salt with gold electrode: (———) first cycle, and (– – –) second cycle. Results from EQCM studies of PC/$LiAsF_6$ solutions (gold electrodes on quartz) are also shown (mass per electron accumulated vs. potential).

from EQCM studies. The use of FT-IR spectroscopy and EQCM enabled the mapping of various surface reactions occurring as a function of the potential applied. Traces of O_2 and H_2O are irreversibly reduced during the first cathodic scan to lithium oxides and LiOH at 2 and 1.5 V, respectively. Gradual salt anion reduction occurs at potentials below 1.8 V (depending on the salt anion; for instance, the $-SO_2CF_3$ group and PF_6^- are reduced at higher potentials than AsF_6^- or ClO_4^-). Alkyl carbonates and esters are reduced below 1.5 V and ethers are reduced below 1 V (Li/Li^+) [6–8]. The use of EQCM in conjunction with linear sweep voltammetry for the study of surface film formation in commonly used lithium battery electrolyte solutions is also demonstrated in Fig. 3 and was discussed in detail in a recent publication [15].

In brief, the change in the resonance frequency (Δf) of the quartz crystal to which the working electrode (noble metal) is attached is proportional to the mass accumulating (Δm) on the electrode due to the electrochemical process (surface film formation at low potentials, lithium deposition and stripping, etc.). Hence, $-\Delta f = C_f \Delta m$ where C_f is a coefficient which depends on the properties of the quartz crystal. The mass per electron (*mpe*) accumulating on the electrode is thus calculated from: $mpe = (d\Delta f/dQ)(F/C_f)$ where Q is the charge involved and F is the Faraday number.

In a voltammetric experiment the charge involved as a function of the potential applied (E) is calculated from i (current density) and v (sweep rate), and thereby *mpe* $(E) = [d\Delta f/dE(E)]\, vF/iC_f$. The *mpe* values thus calculated may be identical to the average equivalent weight of the surface species precipitating on the electrode, provided that the formation of stable surface films is the major electrochemical process taking place. As a result, EQCM may serve as an important analytical tool for identification of the various surface species precipitating at different conditions (e.g.

solution composition and the potential applied). For instance, in Fig. 3, *mpe* values calculated for gold electrodes in three different $LiAsF_6$/PC solutions (as indicated) in linear sweep voltammetry are plotted as a function of the potential applied.

The *mpe* values at ~2 V (Li/Li^+) which are in the 30–35 range may indicate traces of O_2 reduced to LiO_2 and Li_2O_2 at this potential [6]. The *mpe* values between 40 and 55 calculated for 1 M $LiAsF_6$ solutions at ~0.5–0.8 V may indicate a solvent reduction to a combination of $CH_3CH(OCO_2Li)CH_2OCO_2Li$ and Li_2CO_3 (*mpe* = 88 and 37, respectively) as indicated by previous spectroscopic studies [6,8]. The *mpe* values calculated for the 1.5–0.5 V potential domain in 0.25 M $LiAsF_6$ solutions are much lower than in 1 M $LiAsF_6$ solutions. This may indicate a partial dissolution of the solvent and salt reduction products because the lower concentration of the lithium cation may allow their higher solubility in PC. Hence, these experiments enable the examination of the stability of the surface species formed on noble electrodes in different solutions and the order of their sedimentation as a function of the potential applied as well as other experimental conditions. A combination of these EQCM measurements and impedance spectroscopic studies of noble metal electrodes on which surface films were deposited in different solutions (by polarization to low potentials) enabled a stability ladder to be set up for the surface films formed on the electrodes as a function of the potential applied, the solvents, salts and contaminants. This was made possible by following changes in the impedance spectra measured at open-circuit voltage (OCV) from electrodes held at open circuit after film formation [16]. For instance, the films formed in $LiAsF_6$/PC solutions are much more stable than those formed in $LiClO_4$, $LiPF_6$ and $LiBF_4$ solutions in PC. In addition, the surface films formed in EC–DEC solutions are indeed much less stable than those formed in PC or in EC–DMC solutions.

The importance of the above studies of noble metal electrodes in solutions lies in the similarity between the surface films developed on lithium and those developed on noble metals polarized to low potential in the same solutions. Since the driving force for the surface film formation on lithium is continuous, it is impossible to investigate the stability of these surface films as they are constantly formed in cases where a steady state is not obtained (e.g. when the surface species are partially soluble). When these surface films are deposited on the noble metals at low potentials, it is possible to follow their stability and ageing at open circuit using FT-IR [6,8,12], impedance [16] and EQCM techniques [15].

3.4. Lithium–carbon electrodes

We chose to work with synthetic graphite as the model carbon material because the degree of lithium intercalation (up to an optimum of LiC_6), its reversibility and the stability of graphite are the most dependent on the solution composition, compared with other carbons. The correlation between the 3D structure of this carbon and the intercalation level and its reversibility may be relatively easily be followed by in situ XRD. The surface chemistry of these electrodes in solution and the surface films formed were rigorously studied by FT-IR (diffuse reflectance), EDAX and XPS. In general, the surface films developed on the graphite particles at low potential have a similar composition to those developed on lithium (see Scheme 1). However, because of their high area, the role of contaminants such as HF (in the case of $LiPF_6$, $LiBF_4$) is much less pronounced and thereby the above-mentioned ageing processes are less important, i.e. even in $LiPF_6$ solutions the surface chemistry may be dominated by solvent reduction. Graphite can intercalate reversibly with lithium and be cycled hundreds of times in alkyl carbonates and some ethers (e.g. 2Me-THF) containing EC as a co-solvent. The highest stability is obtained in EC–DMC solutions. This is due to the high stability of the surface films formed, comprising the EC reduction product $(CH_2OCO_2Li)_2$ as the major constituent, in this solvent combination. Special attention was given to the study of destruction processes of graphite upon lithium intercalation which limit their stability. The key point is the nature of the surface films formed and their ability to protect the graphite from cracking due to solvent cointercalation. Fig. 4 describes three situations of Li–graphite electrodes as a function of the solution composition and schematic chronopotentiograms of graphite electrodes in these three types of solutions.

In EC-containing solutions of co-solvents such as DMC, DEC and 2Me-THF compact, well passivating and stable surface films are formed (mostly EC reduction products) at potentials high above those of lithium intercalation in graphite (≈250 mV versus Li/Li^+) and protect the graphite particles from any destructive process. The charge involved in the film-forming process is usually about 20% of the total reversible charge (depending on the electrode surface area). A similar situation occurs in CO_2-containing solvents including DMC, DEC, THF, 1,3-dioxolane, 2Me-THF, methyl formate (MF) and γ-butyrolactone (BL) due to the formation of Li_2CO_3 films [1–5]. In solutions based on DMC, THF, MF or BL reduction of solution species at potentials below 1 V does not form efficient passivating films. We have evidence that there are also some changes in the graphite structure which occur simultaneously with these reduction processes. The processes may involve partial exfoliation of the graphite which increases its surface area [17]. Thereby, the charge involved in the reduction of the solution species when the electrodes are polarized first to low potentials is high. The electrode's impedance is thus high and non-uniform (Fig. 4, middle). It is difficult to fully charge these electrodes with lithium galvanostatically (even at low current densities) because the electrode may reach lithium deposition potentials before it is fully intercalated with lithium. In extreme cases such as graphite electrodes in PC solutions (Fig. 4, bottom), the destructive processes of these electrodes result from co-intercalation of solvent molecules and exfoliation and

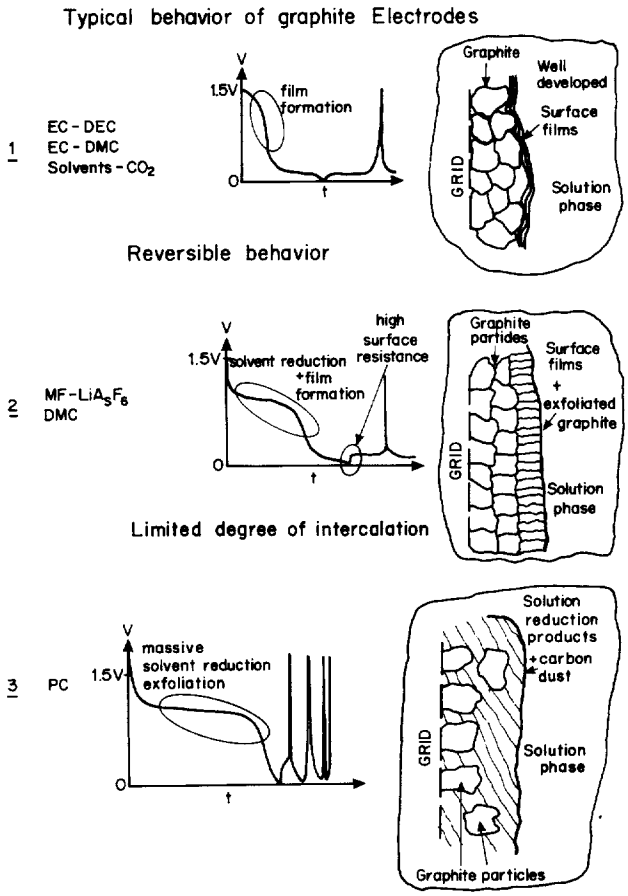

Fig. 4. Typical chronoamperometric behaviour and schematic view of the structure of graphite electrodes in three classes of electrolyte systems. The graphite particles are usually thin flakes and the amorphous parts in 2 and 3 are much thinner than as appearing in the sketch. The particles' thickness and the amorphous regions in 2 and 3 were exaggerated in the figure.

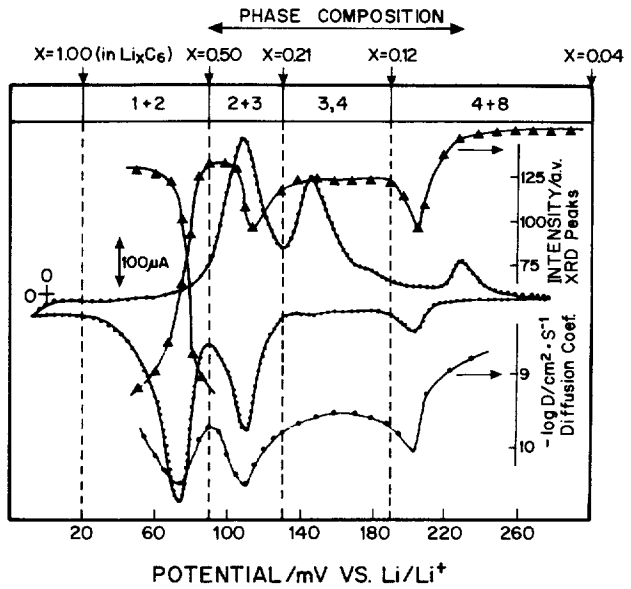

Fig. 5. A comparison of the diffusion coefficient of lithium in graphite (calculated from PITT) intensity of the XRD peaks and cyclic voltammetry as a function of the degree of intercalation [19].

cracking of graphite particles followed by their electrical disconnection from the bulk.

Another important direction of the research was a parallel study of thin film graphite electrodes (a few μm thick on a copper substrate) by slow scan cyclic voltammetry, impedance spectroscopy and potentiostatic intermittent titration [18]. The diffusion coefficient of lithium in graphite as a function of the potential applied (and hence, the degree of intercalation) was determined and found not to be monotonous. There is an interesting correlation between the D versus E, X (Li_xC_6) functions (location of minima and maxima), the intensity of the XRD peaks, the Li–C phases existing and the cyclic voltammetry peaks [19]. Fig. 5 presents this correlation which is an important clue for the understanding of the intercalation mechanism. However, a detailed discussion of this is beyond the scope of this review.

When the carbons used are either disordered material or even graphitized carbons with some turbostratic disorder, they are less sensitive to the solution composition because exfoliation of graphene planes does not readily occur, and hence their stability is not so dependent on the surface chemistry developed. Indeed, these carbons can be cycled in PC solutions in which synthetic graphite cannot reach reversible intercalation at all. It is clear though that solutions which are good for graphite electrodes, in which stable and protective surface films are formed, should also prove excellent for disordered carbons anodes, especially for achieving prolonged cycle life.

References

[1] D. Aurbach, O. Chusid, Y. Carmeli, M. Babai and Y. Ein-Eli, *J. Power Sources, 43* (1993) 47.
[2] D. Aurbach, Y. Ein-Eli, O. Chusid, M. Babai, Y. Carmeli and H. Yamin, *J. Electrochem. Soc., 141* (1994) 603.
[3] D. Aurbach, Y. Ein-Eli, B. Markovsky, Y. Carmeli, H. Yamin and S. Luski, *Electrochim. Acta, 39* (1994) 3669.
[4] D. Aurbach and Y. Ein-Eli, *J. Electrochem. Soc., 142* (1995) 1746.
[5] D. Aurbach, Y. Ein-Eli, B. Markovsky and A. Zaban, *J. Electrochem. Soc., 142* (1995) 2882.
[6] D. Aurbach, M.L. Daroux, P. Faguy and E.B. Yeager, *J. Electroanal. Chem., 297* (1991) 225.
[7] D. Aurbach, *J. Electrochem. Soc., 136* (1989) 906; 1606; 1610; 3198.
[8] D. Aurbach and O. Chusid, *J. Elecrochem. Soc., 138* (1991) L6; *140* (1993) L1; L155.
[9] D. Aurbach and A. Zaban, *J. E; ectrochem. Soc., 142* (1995) L108.
[10] D. Aurbach and Y. Ein-Eli, *J. Electrochem. Soc., 142* (1995) 1746.
[11] D. Aurbach and Y. Cohen, *J. Electrochem. Soc., 143* (1996) 3525.
[12] D. Aurbach, Y. Gofer, M. Ben-Zion and P. Aped, *J. Electroanal. Chem., 339* (1992) 451.
[13] D.R. Louder and B.A. Parkinson, *Anal. Chem., 66*, (1994) 84R; J. Frimer, *Ang. Chem. Int. Ed. Engl., 31* (1992) 1298.

[14] D. Aurbach and Y. Cohen, *J. Electrochem. Soc.*, (1997) in press.
[15] D. Aurbach and A. Zaban, *J. Electroanal. Chem.*, *393* (1995) 43.
[16] D. Aurbach and A. Zaban, *J. Electrochem. Soc.*, *141* (1994) 1808.
[17] D. Aurbach, M. Levi, E. Levi and A. Scheckter, *J. Phys. Chem.*, *101B* (1997) 2195..
[18] W. Weppner and R.A. Huggins, *Ann. Rev. Mater. Sci.*, *8* (1978) 269; C.J. Wen, B.A. Boukamp, R.A. Huggins and W. Weppner, *J. Electrochem. Soc.*, *126* (1979) 2258.
[19] D. Aurbach, M. Levi and E. Levi, *J. Electroanal. Chem.*, *421* (1997) 79; 89.